Preliminary analysis of the interacting pentad bands (ν 2 + 2 ν 4 , ν 2 + ν 3 , 4 ν 2 , ν 1 + 2 ν 2 , 2 ν 1) of CF4 in the 1600 − 1800 cm − 1 region

Manel Mattoussi, M. Rey, M. Rotger, A.V. Nikitin, I. Chizhmakova, Xavier Thomas, H. Aroui, S. Tashkun, Vladimir G. Tyuterev

Version of Record: https://www.sciencedirect.com/science/article/pii/S0022407318308756
Manuscript_059bf992d796839ed9243434d671b09e

Preliminary analysis of the interacting pentad bands ($\nu_2 + 2\nu_4, \nu_2 + \nu_3, 4\nu_2, \nu_1 + 2\nu_2, 2\nu_1$) of CF_4 in the 1600−1800 cm^{-1} region

M. Mattoussi, M. Rey*, M. Rotger

GSMA, UMR CNRS 7331, University of Reims Champagne Ardenne, Moulin de la Housse B.P. 1039, F-51687, Cedex Reims, France

A. V. Nikitin

Laboratory of Theoretical Spectroscopy, Institute of Atmospheric Optics, Russian Academy of Sciences, 634055 Tomsk, Russia

I. Chizhmakova

Laboratory of Quantum Mechanics of Molecules and Radiative Processes, Tomsk State University, 36 Lenin Avenue, 634050 Tomsk, Russia

X. Thomas

GSMA, UMR CNRS 7331, University of Reims Champagne Ardenne, Moulin de la Housse B.P. 1039, F-51687, Cedex Reims, France

H. Aroui

LDMMP, ENSIT, University of Tunis, 5 Av Taha Hussein, 1008 Tunis, TUNISIA

S. Tashkun

Laboratory of Theoretical Spectroscopy, Institute of Atmospheric Optics, Russian Academy of Sciences, 634055 Tomsk, Russia

Vl. G. Tyuterev

GSMA, UMR CNRS 7331, University of Reims Champagne Ardenne, Moulin de la Housse B.P. 1039, F-51687, Cedex Reims, France

Laboratory of Quantum Mechanics of Molecules and Radiative Processes, Tomsk State University, 36 Lenin Avenue, 634050 Tomsk, Russia

Abstract

The Fourier transform spectrum of CF_4 in the 1600-1800 cm^{-1} was recorded in Reims by using a White-type multi-pass cell to provide a path length of 8.262 m. In the present work, all spectrum analyses and fits were realized using the MIRS software based on tetrahedral tensorial formalism. By combining non-empirical contact transformation Hamiltonians for line positions and *ab initio* ro-vibrational normal-mode predictions for line intensities, we are able to achieve a simultaneous fit of effective Hamiltonian and dipole moment parameters of several cold and hot

bands of CF_4. Hamiltonian operator was expanded up to the sixth order for the ground state and for the $\{\nu_2 + 2\nu_4, \nu_2 + \nu_3, 4\nu_2, \nu_1 + 2\nu_2, 2\nu_1\}$ pentad. 1831 line positions were fitted to RMS of 1.5 10^{-3} cm^{-1}. The standard deviation for line intensities for the cold bands $\{\nu_2+2\nu_4, \nu_2+\nu_3, 4\nu_2, \nu_1+2\nu_2, 2\nu_1\}$ is of 1.1 % and of 8 % and 5 % for the hot band transitions $\{2\nu_2 + 2\nu_4 - \nu_2, 2\nu_2 + \nu_3 - \nu_2\}$ and $\{\nu_2 + 3\nu_4 - \nu_4, \nu_2 + \nu_3 + \nu_4 - \nu_4\}$, respectively.

Keywords:
CF_4, Tensorial formalism, *ab initio*, Infrared spectrum, Line positions and intensities

1. Introduction

Tetrafluoromethane CF_4 appears to be of vast industrial, environmental and economical interest. For these reasons, the ro-vibrational spectroscopy of this molecule was a subject of several theoretical and experimental studies. CF_4 belongs to the group of perfluorocarbons (PFCs) which designates the chemicals composed of carbon and fluorine only. These species predominantly CF_4 are extremely stable, inoffensive for the stratospheric ozone layer but powerful greenhouse gases (GHGs). This molecule is found among the longest-lived atmospheric trace gases because of its great chemical stability with an estimated lifetime of more than 50,000 years[1, 2]. In addition, it seems to be the most abundant PFC in the stratosphere. Infrared high spectral resolution solar occultation spectrometer lead to an abundance of 70.45 ±3.40 ppt [3]. Because of this atmospheric persistence, CF_4 is regulated by the Kyoto Protocol of the United Nations Framework Convention on Climate Change (UNFCCC) [4, 5, 6] as a substance whose atmospheric concentration should be supervised and reduced. Besides its natural origin[7, 8, 9], the second source of CF_4 is linked to aluminium production and to the manufacturing of semiconductor[10]. The spectroscopic databases like HITRAN [11, 12] or GEISA [13, 14] only contain a limited range of data for CF_4, without intensity analysis. The spectroscopy of CF_4 which is essential for quantitative measurement in the atmosphere still remains relatively poorly studied because of the complexity of analyses. Some detailed high-resolution studies exist, however they mostly concern line positions. This was the case of the analysis of the ν_3 fundamental with the $2\nu_3$ overtone[15] and the interaction of this stretching state with the $2\nu_4$ overtone[16]. Recent work was already dedicated to the analysis of some rovibrational bands of this molecule including some hot bands around 1283 cm^{-1}[17], the data being included in the Dijon database [18]. First accurate and complete *ab initio* based line lists for CF_4 up to 400 K in the range 0-4000 cm^{-1} have been recently published by the Reims-Tomsk groups [19], resulting in 2 billion rovibrational transitions. In Ref.[19], although the variationally-predicted were not computed at the spectroscopic accuracy, the error on line intensities was only of few % allowing a correct global description of the overtones and combination bands up to 6 vibrational quanta validated by direct comparisons with experimental PNNL spectra.
In this work, we report the analysis of rovibrational interacting pentad bands ($\nu_2 + 2\nu_4, \nu_2 + \nu_3, 4\nu_2, \nu_1 + 2\nu_2, 2\nu_1$) of this molecule, in order to obtain a reliable simulation of CF_4'atmospheric absorption in the region between 1600-1800 cm^{-1}, including the most significant hot bands. The study of this system of bands requires the investigation of various vibrational fundamentals, combinations and harmonics bands. For the first time, high resolution analysis was made

*Tel. (33)-3-26-91-33-06 ; fax: (33)-3-26-91-31-47
Email address: michael.rey@univ-reims.fr (M. Mattoussi, M. Rey*, M. Rotger)

by combining spectroscopic effective models and information provided by accurate *ab initio* potential energy (PES) and dipole moment (DMS) surfaces both for line positions and line intensities.A non-empirical effective Hamiltonian was built from a PES by applying high-order contact-transformations (CT) [20, 21]. For the line intensities, some effective dipole moment parameters have been adjusted directly on the *ab initio* intensities [19]. Section 2 describes the experimental data used, while Section 3 reviews some basic principles concerning the theoretical model for tetrahedral molecules used for our analysis and presents the obtained results.

2. Experimental details

Spectra measurements were carried out with the Fourier Transform Spectrometer (FTS) of GSMA laboratory [22]. The CF_4 spectrum was recorded at room temperature over the range 1600-1800 cm^{-1}, with a spectral resolution of 0.003 cm^{-1} (maximum optical path length of 2.99 m). This experimental setup was equipped with a globar source, a CaF_2 beam splitter and a HgCdTe detector. A White-type multi-pass cell with a basis length of 2m was used to provide a path length of 8.262 m. The pressure in the cell was maintained at 9.93 Torr. The spectrum was obtained by co-adding and averaging 289 one-sided interferometer scans in order to achieve a sufficient signal-to-noise ratio. The diaphragm diameter was set to 4.5 mm. Wavenumber calibration was carried out using residual of ten water lines with intensities in the range 2×10^{-19} - 2×10^{-20} cm/molecule.
The detailed experimental conditions are listed in Table 1, and an overview of transmittance spectrum of the $(\nu_2 + 2\nu_4, \nu_2 + \nu_3, 4\nu_2, \nu_1 + 2\nu_2, 2\nu_1)$ pentad is plotted in Figure 1.

3. Spectra analysis and modeling

3.1. Theoretical methods

The aim of the present work is the detailed analysis of the pentad system composed of five bands, namely $\nu_2 + 2\nu_4$, $\nu_2 + \nu_3$, $4\nu_2$, $\nu_1 + 2\nu_2$ and $2\nu_1$ in the spectral range 1600-1800 cm^{-1} using a specific spectroscopic model (see also section 4.2), t. The absorption in this range is dominated by ν_2+ν_3 with the band center near 1717 cm^{-1}. The complexity of CF_4 vibrational states is outlined in Figure 2 where the scale on the right panel represents sublevel with their symmetry type of the pentad split into 14 different components. The ν_2+$2\nu_4$ vibrational band has 6 vibrational sublevels of A_1, A_2, $2E$, F_1 and F_2 symmetry types, the ν_2+ν_3 band has 2 sublevels (F_1, F_2), $4\nu_2$ has 3 sublevels of symmetry A_1 and $2E$, $\nu_1 + 2\nu_2$ has 2 sublevels (A_1, E) and $2\nu_1$ has one upper state vibrational level of A_1 symmetry.
The infrared tetrafluoromethane spectra are known to be very complex due to the high tetrahedral symmetry of CF_4 which causes degeneracies and quasi-degeneracies of the vibration modes and large and complicated resonance interactions because of the inter-modes coupling. Note that such a line-by-line analysis from a judicious combination of effective and *ab initio* models−both for line positions and line intensities−was not yet available in this spectral interval. In order to extend rovibrational analyses of experimental spectra, we used a tensorial formalism with vibrational extrapolation [23, 24] including supplementary information derived from *ab initio* PES/DMS and first-principles calculations. These *ab initio* variational line lists are available in the TheoReTS information system [25]. Significant recent advance in *ab initio* PES, DMS and in rotationally resolved variational spectra calculations reported by Rey *et al.* [19] permitted

identification of the most important bands in this range. But, many weak transitions remained not yet assigned.

The rovibrational model for line-by-line analysis is built by admitting that the vibrational energy levels of CF_4 can be gathered in a series of polyads. In the framework of this theory, an effective Hamiltonian (EH) for all the considered polyads was constructed from high-order contact transformations (CT) to eliminate inter-polyad interaction terms in the rovibrational Hamiltonian (transform completely the Hamiltonian to a block-diagonal form) [20, 21]. This approach allows a fairly precise characterization of resonance coupling terms to avoid the ambiguity of purely empirical EH models [26, 27]. The effective Hamiltonian operator $\widetilde{H}$ adapted to the polyad structure of the CF_4 is constructed as the sum of contributions appropriate to the various polyads designed by P_k (k=0, 1, ..., k, ...), P_0 being the ground state (GS). This effective Hamiltonian is expressed as (see Figure 2)

$$\widetilde{H} = \sum \widetilde{H}_{\{P_k\}} = \widetilde{H}_{\{P_0\}} + \widetilde{H}_{\{P_1\}} + ... + \widetilde{H}_{\{P_k\}} + ... \tag{1}$$

$$= \widetilde{H}_{\{P_0\}} + \widetilde{H}_{\{\nu_2\}} + \widetilde{H}_{\{\nu_4\}} + \widetilde{H}_{\{Dyad1\}} + \widetilde{H}_{\{\nu_2+\nu_4\}} + \widetilde{H}_{\{Tetrad\}} + \widetilde{H}_{\{Dyad2\}} + \widetilde{H}_{\{Pentad\}}$$

The terms of this expansion gather operators specific to the successive polyads in the representation of the irreducible tensor operators (ITO) [24, 28, 29]. They are written as a linear combination of rovibrational operators $T^{\Omega(K,n\Gamma_r)\Gamma_1\Gamma_2\Gamma_v}_{\{n_s\}\{m_s\}}$ as

$$\widetilde{H}_{\{P_k\}} = \sum_{\text{all indices}} t^{\Omega(K,n\Gamma_r)\Gamma_1\Gamma_2\Gamma_v}_{\{n_s\}\{m_s\}} T^{\Omega(K,n\Gamma_r)\Gamma_1\Gamma_2\Gamma_v}_{\{n_s\}\{m_s\}}. \tag{2}$$

In this equation, the t's are the corresponding adjustable parameters to be determined. All the indices represent the intermediate quantum numbers and symmetries. Here T refers to a rovibrational operator expressed as a tensor product between rotational and vibrational operators as

$$T^{\Omega(K,n\Gamma_r)\Gamma_1\Gamma_2\Gamma_v}_{\{n_s\}\{m_s\}} = \beta \left(R^{\Omega(K,n\Gamma_r)} \otimes {}^{\varepsilon} V^{\Gamma_1\Gamma_2\Gamma_v}_{\{n_s\}\{m_s\}} \right)^{(A_1)}. \tag{3}$$

Rotational operators $R^{\Omega(K,n\Gamma_r)}$ are the usual symmetry-adapted irreducible tensor operators (ITO) for spherical top molecules [23, 24, 30, 31, 32, 33, 34]. The upper index Ω is the rotational degree in the molecular frame components J_x, J_y and J_z; K is the tensor rank relative to the full rotation group $O(3)$, n is a multiplicity index and Γ_r (=A_1, A_2, E, F_1 or F_2) is the rotational symmetry in the T_d point group. The vibrational ITOs are constructed by recursive coupling of elementary creation a^+ and annihilation a operators for each of the four normal modes. ε is the parity in conjugate momenta with the condition $\varepsilon = (-1)^{\Omega}$ and Γ_1 and Γ_2 are the symmetries of vibrational operators; n_s and m_s are the degrees in the a^+ and a operators. Here, β is a numerical factor, equal to $[\Gamma_1]^{1/2}(-\sqrt{3}/4)^{\Omega/2}$ if $(K, n\Gamma_r) = (0, 0A_1)$, and 1 otherwise. Since the Hamiltonian is totally symmetric, we have necessary $\Gamma_r = \Gamma_v$. The order of the individual terms in T is defined as $\sum_s (n_s + m_s) + \Omega - 2$. Orientation of the ITOs in the chain $O(3) \supset T_d$ has been described in details in Ref. [35].

In order to perform intensity calculation, the dipole moment operator is built in the same way as the effective Hamiltonian operator. Its components μ_Θ ($\Theta = X, Y$ or Z) in the laboratory fixed frame (LFF) are linked to the components μ_θ ($\theta = x, y$ or z) in the molecule fixed frame (MFF) as

$$\mu_\Theta = \sum_\theta \lambda_{\Theta\theta}\mu_\theta, \tag{4}$$

where $\lambda_{\Theta\theta}$ are the direction cosines. The transformed LFF components can be expressed in terms of the MFF transformed components as

$$\widetilde{\mu}_\Theta = \frac{1}{2}\sum_\theta (\lambda_{\Theta\theta}\widetilde{\mu}_\theta + \widetilde{\mu}_\theta\lambda_{\Theta\theta}), \tag{5}$$

where the MFF effective dipole moment is of symmetry F_2 with its three components $\widetilde{\mu}_\theta$ expanded as a series of rovibrational operators [23, 36]

$$\widetilde{\mu}_\theta^{(F_2)} = \sum_{\{i\}} \widetilde{\mu}^{\{i\},\Gamma} \left(R^{\Omega(K,n\Gamma_r)} \otimes {}^{\varepsilon}V^{\Gamma_1\Gamma_2\Gamma_v}_{\{n_s\}\{m_s\}} \right)^{(F_2)}_\theta . \tag{6}$$

Here $\widetilde{\mu}^{\{i\},\Gamma}$ are the effective dipole moment parameters to be determined. A way to determine these parameters will be described in the section 3.2.2. Note that the order of the individual terms of the dipole moment is $\sum_s (n_s + m_s) + \Omega - 1$.

3.2. Analysis and discussion

3.2.1. Line positions

Line-by-line analysis and assignments of experimental spectra are known to be tedious and difficult tasks. They are usually based on empirical models for the polyads of close states where line positions are generated from empirically-fitted effective Hamiltonians (EH). Using a vibrational extrapolation scheme, we simulate the spectrum by considering the polyad P_0, which contains the GS level and the polyad P_7 containing the ν_2+2ν_4, ν_2+ν_3, 4ν_2, ν_1+2ν_2 and 2ν_1 levels as the upper polyad. To obtain a result with a precision comparable with the experimental accuracy, the effective Hamiltonian was expanded up to the sixth order. As a starting point, we needed a first estimation of the tensorial parameters. That permitted a correct description of the experimental spectrum at a given temperature. Starting with the best possible set of parameters permits to identify a large number of observed line positions. Here as a first guess, the *ab initio* based EH parameters obtained via the CT method were used and further refined after various iterations by increasing the number of assigned lines. This supplied realistic estimations for the rovibrational coupling parameters between various bands of a given polyad that are responsible for the intensity perturbations due to accidental resonances. This first set of parameters allowed a preliminary simulation. In what follows, parameters for ν_2, ν_4, (2ν_2, ν_1) dyad, ν_2+ν_4, (2ν_4, ν_3, 3ν_2, ν_1) tetrad and (2ν_2+ν_4, ν_1+ν_4) dyad states will be fixed to the "*ab initio*" values derived from CTs. That means that only the parameters for the ground state and (ν_2+ν_4, ν_2+ν_3, 4ν_2, ν_1+2ν_2, 2ν_1) are adjusted. Spectrum simulations, line assignments and the fitting process were carried out using the MIRS [37, 38] and SpectrAssign softwares based on an iterative semi-automatized comparison of synthetic and experimental spectra. The T_d formalism is implemented in MIRS that thus provides all vibrational and rotational quantum numbers. The SpectrAssign program was used for assignments and visualization. It allows a simultaneous display of predicted lines from MIRS output and of an experimental spectrum. A limited number of observed lines were assigned by comparing the positions and intensities of the observed and simulated lines calculated from the initial values of the spectroscopic parameters. Afterwards, new assignments were made leading to a new set of fitted tensorial parameters. This process was performed iteratively

until no more lines could be assigned.
Finally, among the 618 parameters included in the sixth order effective Hamiltonian, only 48 have been fitted. The root mean square (RMS) deviation of the IR data is very satisfactory. In Figure 3, we present an overview of the pentad region. It compares the observed spectrum with the calculated one at the same experimental conditions by using our final set of parameters in the region 1600–1800 cm^{-1} dominated by the $\nu_2+\nu_3$ combination band. As shown in this figure, calculated and observed spectra are in very good agreement. As can be seen in Figure 4, different zooms reveal the precision obtained of calculated positions in the *R* and *P*-branches though weaker lines belonging to hot bands need to be still improved. Note that the *Q*-branch has an unresolved structure due to a tremendous number of overlapping lines making assignments very complicated. In order to keep the total number of adjusted parameters reasonable and to make the model "stable" when slightly changing parameters, an important part of the non-diagonal resonance parameters have been kept fixed to their theoretical values generated from the PES [19] in a manner similat to that described for the methane molecule [23]. Although the *ab initio* values for non-diagonal parameters are approximations, they describe the resonance couplings in a quite qualitatively correct way. On the other hand, an empirical "blind" fitting of a big set of effective polyad Hamiltonian parameters to rovibrational energies is known as a mathematically poorly defined inverse problem [26, 27]. Purely empirical approach could improve a root-mean-square deviation on line positions, but it often results in wrong values of interaction parameters and thus wrong intensity extrapolations. The accurate theoretical calculations of resonance coupling parameters from *ab initio* PES and of the corresponding intensities are difficult tasks.

According to this preliminary study, we were able to assign 1831 line positions, belonging mainly to the $\nu_2+\nu_3$ combination band, with a root mean square deviation of 1.590×10^{-3} cm^{-1}. Nevertheless, a large part of the transitions remained unassigned. A complete modelling of all bands in this region will require more assignments of both hot and cold transitions. Number of assigned transitions per band depends on the inherent intensity of the band and on the degree of interaction with other states. Figure 5 shows the residual defined by the difference between the observed and calculated wavenumbers versus J. It gives a global idea of the quality of the fit. We note that the data are well distributed on the scale of the J values. It allowed to make sure that the rovibrational energy levels are well sampled and that the results of the fit are reliable. Figure 6 presents the resulting calculated reduced upper state energies vs J showing the mixtures between the vibrational sub-levels.

3.2.2. Line intensities

Tetrafluoromethane has the same tetrahedral geometry as methane but the main difference is that the CF_4 molecule is heavier and consequently has much lower vibrational modes and much higher J-levels are populated. This leads to a considerable number of IR-active transitions belonging to hot bands that make the experimental spectra more complicated to analyse. Rey *et al.* [19] showed that the CF_4 spectra could be described from (i) a set of strong lines responsible for the strongest absorption features and (ii) of a kind of quasi-continuum formed by an accumulation of very week overlapping lines (see figure of [19]). This situation is quite similar to that observed in hot methane spectra at $\approx$ 1000-1200 K [39]. Because the infrared spectra of CF_4 are very congested, no single line intensity measurements were made. Almost all the observed lines result from overlapping of several transitions. To overcome such a difficulty, we have adopted a strategy quite different from "usual" spectroscopic studies. It consists in fitting the effective dipole moment parameters directly on the variationally-determined *ab initio* intensities. In other words, the variational line list built in Ref. [19] was taken as an "observed" line list for the present

work. To our knowledge, this procedure has never been applied before for such a complex five-atomic molecular system. The improvement of hot bands intensity modelling will be necessary to achieve a more detailed assignment in the region between 1600−1800 cm^{-1} because many other bands belonging to upper polyads e.g. {$2\nu_2$+$2\nu_4$-ν_2, $2\nu_2$+ν_3-ν_2, ν_2+$3\nu_4$-ν_4, ν_2+ν_3+ν_4-ν_4} contribute to the absorption. Detailed statistics on this fit are listed in Table 2. The obtained effective dipole moment parameters for each band summarized in Tables 3, 4 and 5 rely on tensorial formalism notations. Figure 7 presents the resulting comparison between experiment and simulation, with a nice agreement.

4. Conclusion

In this work, we have built a tensorial model that permitted for the first time a detailed analysis of the (ν_2+$2\nu_4$, ν_2+ν_3, $4\nu_2$, ν_1+$2\nu_2$, $2\nu_1$) band system of CF_4 by combining non-empirical CT Hamiltonian, *ab initio* based variational predictions and experimental information. The present analysis supplies a first accurate and complete description of the infrared high-resolution spectrum of CF_4 in the region 1600−1800 cm^{-1}. The final set of effective Hamiltonian/dipole moment parameters allows to reproduce simultaneously (i) quite accurately the cold bands and (ii) in a qualitative manner the main hot band transitions. The global fit of parameters and calculation of infrared spectrum was carried out with the MIRS and SpectrAssign softwares. Assignments was made up to J_{max} = 70 and a set of 48 tensorial parameters has been adjusted. The accuracy of the final empirically optimized calculated line list is satisfactory. We have obtained a root mean square deviation RMS of about 1.590×10^{-3} cm^{-1} for 1831 cold transitions. The standard deviation for line intensities for the cold bands {ν_2+$2\nu_4$, ν_2+ν_3, $4\nu_2$, ν_1+$2\nu_2$, $2\nu_1$} is of 1.1%, with respect to the *ab initio* intensities, while, for the hot bands {$2\nu_2$+$2\nu_4$-ν_2, $2\nu_2$+ν_3-ν_2} and {ν_2+$3\nu_4$-ν_4, ν_2+ν_3+ν_4-ν_4}, the standard deviation is of ≈ 8 % and 5 %, respectively. The main objective of this study was to construct a CF_4 line list for various applications. This final list will include new assignments in the forthcoming versions of the spectroscopic HITRAN and GEISA databases. The line list for the assigned transitions is available as supplementary material to this paper. By using cold spectra (<200 K), future works will consist to both improve the present region and extend analysis to other spectral ranges on the basis of the present results.

References

[1] Ravishankara A, Solomon S, Turnipseed A A and Warren R, Atmospheric lifetimes of long-lived halogenated species, Science 1993;**259**:194-199.

[2] Morris R A, Miller T M, Viggiano A, Paulson, J F,Solomon S and Reid G, Effects of electron and ion reactions on atmospheric lifetimes of fully fluorinated compounds, J Geophys Res Atmos 1995;**100**:1287-1294.

[3] Rinsland C P, Mahieu E, Zander R, Nassar R, Bernath P, Boone C and Chiou L S, Long-term stratospheric carbon tetrafluoride CF_4 increase inferred from 1985–2004 infrared space-based solar occultation measurements, Geophys Res Lett 2006;**33**.

[4] Harnisch J and Höhne N, Comparison of emissions estimates derived from atmospheric measurements with national estimates of HFCs, PFCs and SF_6, Environ Sci Pollut Res 2002;**9**:315-319.

[5] Harnisch J, de Jager D, Gale J and Stobbe O, Halogenated compounds and climate change, Environ Sci Pollut Res 2002;**9**:369-374.

[6] Boudon V, Champion J-P, Gabard T, Pierre G, Loëte M and Wenger C, Spectroscopic tools for remote sensing of greenhouse CH_4, CF_4 and SF_6, Environ Chem Lett 2003;**1**:86-91.

[7] Harnisch J and Borchers R, Effect of natural tetrafluoromethane, Nature 1996;**384**:32.

[8] Harnisch J, Borchers R, Fabian P and Maiss M, Tropospheric trends for CF_4 and C_2F_6 since 1982 derived from SF_6 dated stratospheric air, Geophys Res Lett 1996;**23**:1099-1102.

[9] Deeds D A, Vollmer M K, Kulongoski J T, Miller B R, Mühle J, Harth C M, Izbicki J A and Hilton D R and Weiss, R F, Evidence for crustal degassing of CF_4 and SF_6 in Mojave Desert groundwaters, Geochim Cosmochim Acta 2008;**72**:999-1013.

[10] Khalil M A K, Rasmussen R A, Culbertson J A, Prins J M, Grimsrud E P and Shearer M J, Atmospheric perfluorocarbons, Environ sci technol 2003;**37**:4358-4361.

[11] Rothman L S, Gordon I E, Babikov Y, Barbe A, Benner D C, Bernath P F, Birk M, Bizzocchi L, Boudon V, Brown L R et al., The HITRAN 2012 molecular spectroscopic database, J Quant Spectrosc Radiat Transf 2013;**130**:4-50.

[12] Gordon I E, Rothman L S, Hill C, Kochanov R V, Tan Y, Bernath P F, Birk M, Boudon V, Campargue A, Chance K et al., The HITRAN 2016 molecular spectroscopic database, J Quant Spectrosc Radiat Transf 2017;**203**:3-69.

[13] Jacquinet-Husson N, Crepeau L, Armante R, Boutammine C, Chédin A, Scott N, Crevoisier C, Capelle V, Boone C, Poulet-Crovisier N et al., The 2009 edition of the GEISA spectroscopic database, J Quant Spectrosc Radiat Transf 2011;**112**:2395-2445.

[14] Jacquinet-Husson N, Armante R, Scott A, Chédin A, Crépeau L, Boutammine C, Bouhdaoui A, Crevoisier C, Capelle V, Boonne C et al., The 2015 edition of the GEISA spectroscopic database, J Mol Spectrosc 2016;**327**:31-72.

[15] Gabard T, Pierre G and Takami M, Study of the ν_3 and $2\nu_4$ interacting states of $^{12}CF_4$, Mol Phys 1995;**85**:735-744.

[16] Boudon V, Mitchell J, Domanskaya A, Maul C, Georges R, Benidar, A and Harter W G, High-resolution spectroscopy and analysis of the $\nu_3/2\nu_4$ dyad of CF_4, Mol Phys 2011;**109**:2273-2290.

[17] Carlos M, Gruson O, Richard C, Boudon V, Rotger, M, Thomas X, Maul C, Sydow C, Domanskaya A, Georges R et al., High-resolution spectroscopy and global analysis of CF_4 rovibrational bands to model its atmospheric absorption, J Quant Spectrosc Radiat Transf 2017;**201**:75-93.

[18] Ba Y.A., Wenger C., Surleau R., Boudon V., Rotger M.,Daumont L., et al., MeCaSDa and ECaSDa: Methane and ethene calculated spectroscopic databases for the virtual atomic and molecular data centre, J Quant Spectrosc Radiat Transf 2013;**130**:62-68.

[19] Rey M, Chizhmakova I S, Nikitin A V and Tyuterev Vl G, Understanding global infrared opacity and hot bands of greenhouse molecules with low vibrational modes from first-principles calculations: the case of CF_4, Phys Chem Chem Phys 2018;**20**:21008-21033.

[20] Tyuterev Vl G, Tashkun S A and Seghir H, High-order contact transformations: general algorithm, computer implementation and triatomic tests, SPIE 2004;**5311**:164-176.

[21] Tyuterev Vl G, Tashkun S, Rey M, Kochanov R, Nikitin A V and Delahaye T, Accurate spectroscopic models for methane polyads derived from a potential energy surface using high-order contact transformations, J Phys Chem A 2013;**117**:13779-13805.

[22] Plateaux J, Barbe A and Delahaigue A, Reims high resolution Fourier transform spectrometer. Data reduction for ozone, Spectrochim Acta A Mol Biomol Spectrosc 1995;**51**:1153-1169.

[23] Champion J-P, Loëte M and Pierre G, Spherical top spectra, Spectroscopy of the Earth's atmosphere and interstellar medium 1992:339-422.

[24] Boudon V, Champion J-P, Gabard T, Loëte M, Michelot F, Pierre G, Rotger M, Wenger C and Rey M, Symmetry-adapted tensorial formalism to model rovibrational and rovibronic spectra of molecules pertaining to various point groups, J Mol Spectrosc 2004;**228**:620-634.

[25] Rey M, Nikitin A V, Babikov Y L and Tyuterev Vl G, TheoReTS–An information system for theoretical spectra

based on variational predictions from molecular potential energy and dipole moment surfaces, J Mol Spectrosc 2016;**327**:138-158.
[26] Tyuterev Vl G, Champion J-P, Pierre G and Perevalov V, Fourth-order invariant parameters for F_2 isolated fundamental states of tetrahedral molecules: The study of the ν_4 band of $^{12}CH_4$, J Mol Spectrosc 1984;**105**:113-138.
[27] Perevalov V, Tyuterev Vl G, Zhilinskii B I, Ambiguity of spectroscopic parameters in the case of accidental vibration-rotation resonances in tetrahedral molecules. r^2J and r^2J^2 terms for E-F_2 interacting states, Chem Phys Lett 1984;**104**:455-461.
[28] Nikitin A V, Champion J-P and Tyuterev Vl G, Improved Algorithms for the Modeling of Vibrational Polyads of Polyatomic Molecules: Application to T_d, O_h, and C_{3v} Molecules, J Mol Spectrosc 1997;**182**:72-84.
[29] Rey M, Nikitin A V and Tyuterev Vl G, Ab initio ro-vibrational Hamiltonian in irreducible tensor formalism: a method for computing energy levels from potential energy surfaces for symmetric-top molecules, Mol Phys 2010;**108**:2121-2135.
[30] Champion J-P, Développement complet de l'Hamiltonien de vibration-rotation adapté à l'étude des interactions dans les molécules toupies sphériques. Application aux bandes ν_2 et ν_4 de $^{12}CH_4$, Can J Phys 1977;**55**:1802-1828.
[31] Wenger C and Champion J-P, Spherical top data system STDS software for the simulation of spherical top spectra, J Quant Spectrosc Radiat Transf 1998;**59**:471-480.
[32] Zhilinskii B I, Perevalov V I and Tyuterev Vl G, The method of irreducible tensor operators in the theory of molecular spectra, Novosibirsk Izdatel Nauka 1987.
[33] Moret-Bailly J, Calculation of the frequencies of the lines in a threefold degenerate fundamental band of a spherical top molecule, J Mol Spectrosc 1965;**15**:344-354.
[34] Zhilinskii B I, Reduction of rotational operators to standard form, Opt Spectrosc 1981;**51**:262-263.
[35] Rey M, Boudon V, Wenger C, Pierre G and Sartakov B, Orientation of $O(3)$ and $SU(2) \times C_I$ representations in cubic point groups (O_h, T_d) for application to molecular spectroscopy, J Mol Spectrosc 2003;**219**:313-325.
[36] Papousek D and Aliev M R, Molecular vibrational-rotational spectra, 1982.
[37] Nikitin A V, Champion J-P and Tyuterev Vl G, The MIRS computer package for modeling the rovibrational spectra of polyatomic molecules, J Quant Spectrosc Radiat Transf 2003;**82**:239-249.
[38] Nikitin A V, Rey M, Champion J-P and Tyuterev Vl G, Extension of the MIRS computer package for the modeling of molecular spectra: from effective to full ab initio ro-vibrational hamiltonians in irreducible tensor form, J Quant Spectrosc Radiat Transf 2012;**113**:1034-1042.
[39] Rey M, Nikitin A V and Tyuterev Vl G, Accurate theoretical methane line lists in the infrared up to 3000 K and quasi-continuum absorption/emission modeling for astrophysical applications, Astrophys J 2017;**847**:105.

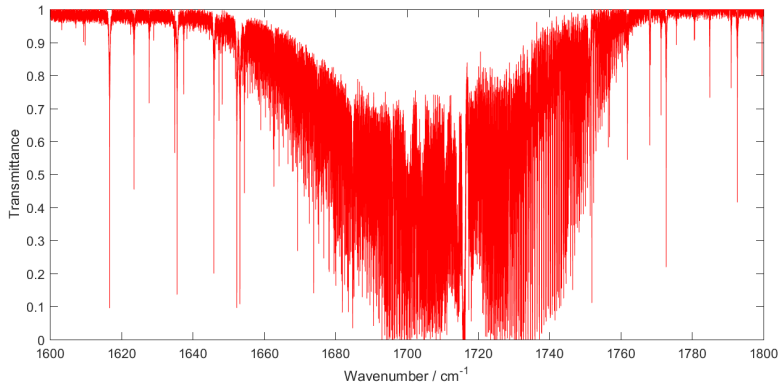

Figure 1: Transmittance spectrum of CF_4, recorded at 294 K at a pressure of 9.93 Torr in the spectral range between 1600 and 1800 cm^{-1}.

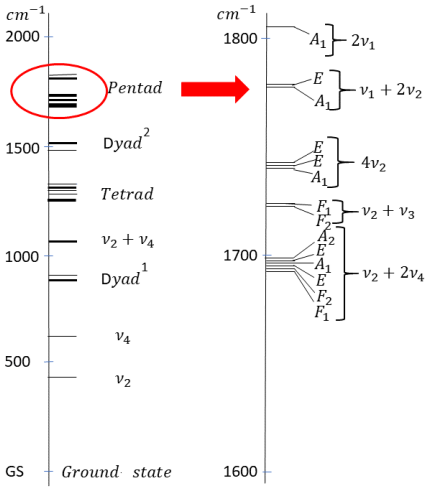

Figure 2: Scheme of vibrational level patterns of the CF_4 polyads (left side) and vibrational sublevels of the part of the pentad system corresponding to ro-vibrational bands analyzed in this work. At the right hand side panel, symmetry type (T_d irreducible representations) of vibration sublevels, vibrational ranking numbers within the pentad and the corresponding vibrational bands are given. The first dyad is composed of [$2\nu_2$, ν_1], the tetrad is composed of [$2\nu_4$, ν_3, $3\nu_2$, $\nu_1+\nu_4$] and the second dyad is composed of [$\nu_1+\nu_2$, $2\nu_2+\nu_4$].

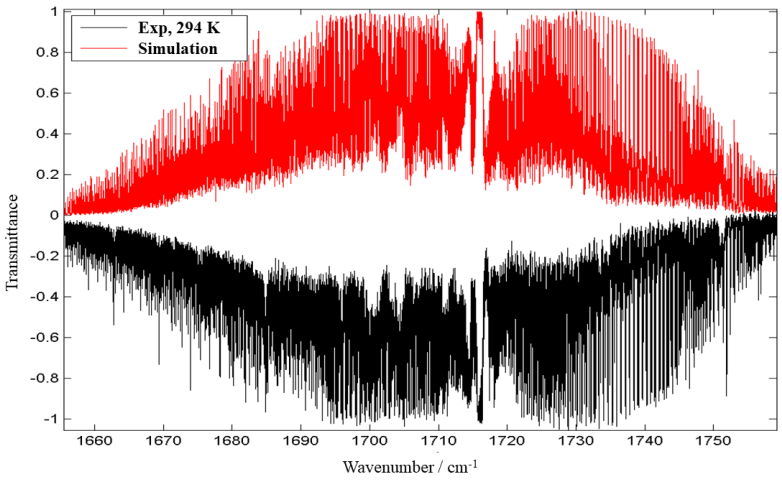

Figure 3: Comparaison between experimental and simulated spectra of CF_4 at 294 K.

Table 1: Experimental details.

Spectral range (cm^{-1})	1600-1800
Resolution (cm^{-1})	0.003
Source	Globar
Separator	CaF_2
Detector	HgCdTe
Cell	White multi-pass
Optical Path (m)	8.262
Temperature (K)	294
Pressure (Torr)	9.93
Aperture diameter (mm)	4.5

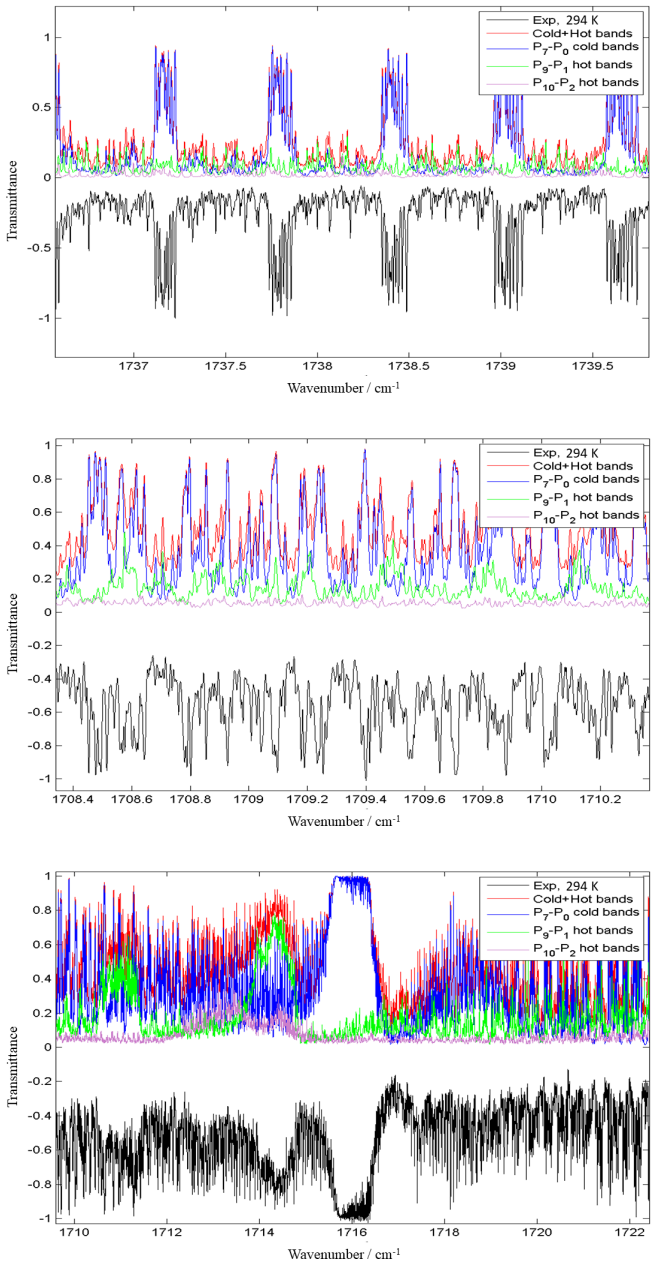

Figure 4: Detailed comparison of the *R*, *P* and *Q*-branches between the observed spectrum and the simulation.

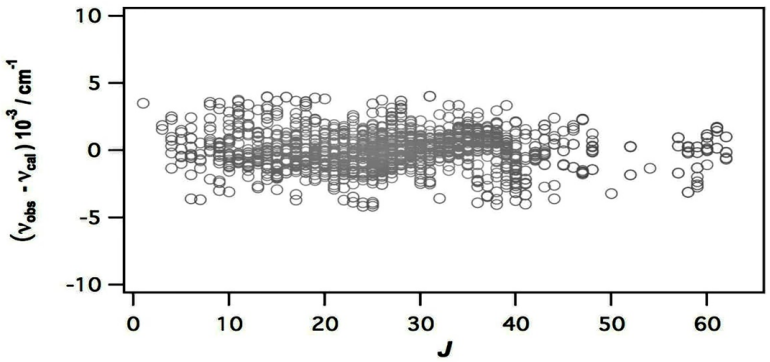

Figure 5: Observed minus calculated wavenumbers versus J for the pentad obtained using the tensorial model. We have a lack of assignments between $J = 50$ and $J = 60$ because of the complexity of the CF_4 spectrum in this region.

Table 2: Summary of the intensity Fit statistics of hot and cold bands.

Bands		J_{max}	Parameters	Assignments	St. Deviation (%)
Hot Bands	$\{2\nu_2+2\nu_4-\nu_2, 2\nu_2+\nu_3-\nu_2\}$	35	28	1871	8
	$\{\nu_2+3\nu_4-\nu_4, \nu_2+\nu_3+\nu_4-\nu_4\}$	30	34	21779	5
Cold Bands	$\{\nu_2+2\nu_4, \nu_2+\nu_3, 4\nu_2, \nu_1+2\nu_2, 2\nu_1\}$	70	16	36896	1.1

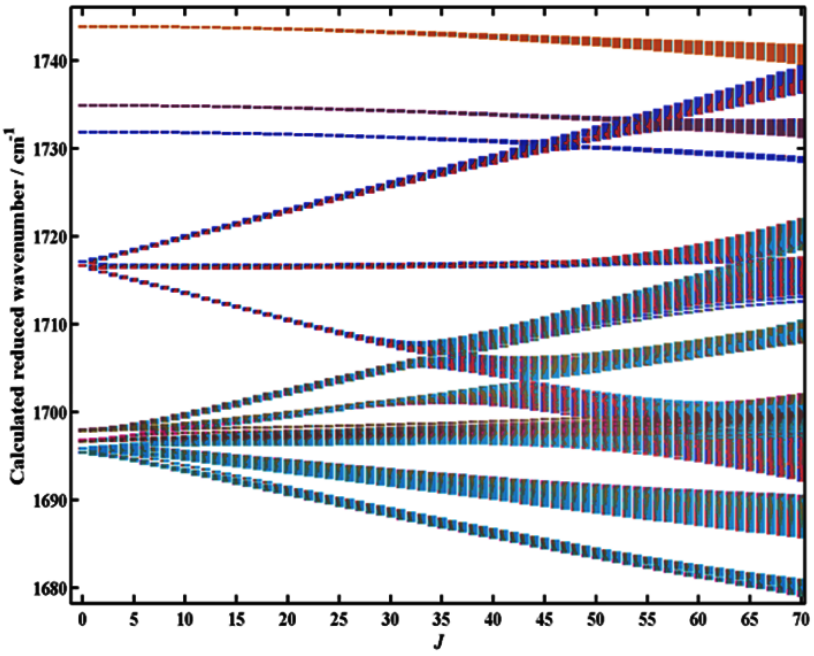

Figure 6: Calculated reduced rovibrational energy levels of CF_4 transitions from 1600 to 1800 cm^{-}1 up to $J = 70$. Various colors correspond to mixing coefficients of normal mode wavefunctions due to resonance interactions.

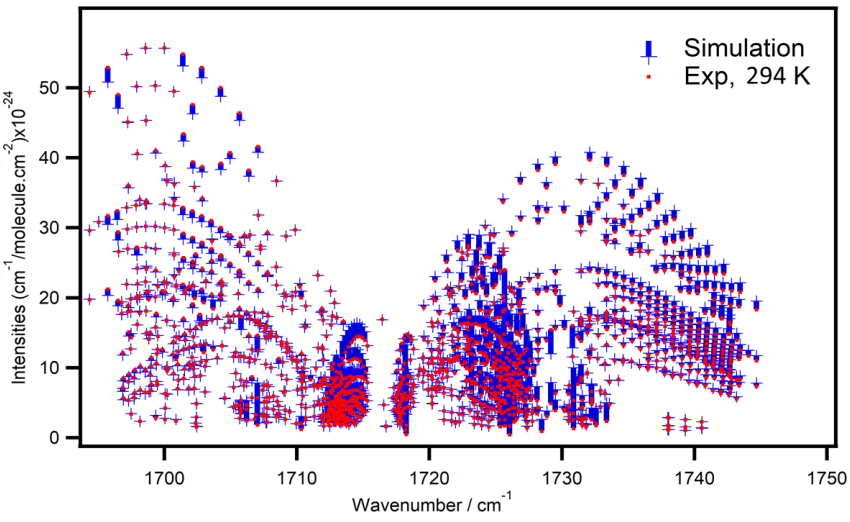

Figure 7: Observed and calculated intensities in (cm^{-1}/molecule.cm^{-2}) vs line positions in (cm^{-1}) for the pentad transitions.

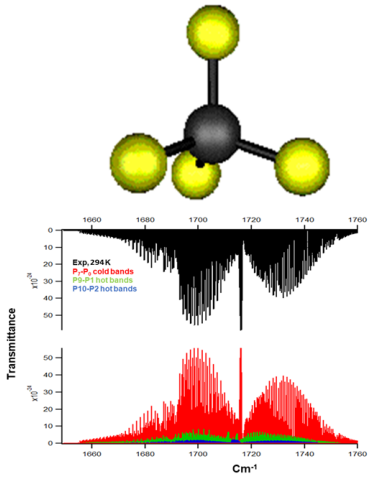

Figure 8: TOC figure: Determination of line positions and line intensities of CF_4 in the region 1600-1800 cm^{-1}.

Table 3: Effective dipole moment parameters for the pentad $\{\nu_2+2\nu_4, \nu_2+\nu_3, 4\nu_2, \nu_1+2\nu_2, 2\nu_1\}$.

	Tensorial nomenclature		Parameter value
	Rotational	Vibrational	
1	R 0(0, 0A_1)	0000 0102	-3.1864538041E-04
2	R 0(0, 0A_1)	0000 0110	9.2315030571E-03
3	R 1(1, 0F_1)	0000 0102	1.2645029053E-06
4	R 1(1, 0F_1)	0000 0102	-1.5390407345E-06
5	R 1(1, 0F_1)	0000 0102	-1.0548647219E-06
6	R 1(1, 0F_1)	0000 0102	1.2126152550E-06
7	R 1(1, 0F_1)	0000 0102	1.5140232527E-06
8	R 1(1, 0F_1)	0000 0110	-1.2529078490E-05
9	R 1(1, 0F_1)	0000 0110	2.2076230400E-05
10	R 1(1, 0F_1)	0000 1200	2.2577731112E-05
11	R 2(2, 0E)	0000 0110	1.5222082012E-08
12	R 2(2, 0F_2)	0000 0110	-1.6089425075E-08
13	R 2(0, 0A_1)	0000 0110	-1.5434076560E-08
14	R 2(2, 0E)	0000 0110	-2.6796194562E-09
15	R 2(2, 0F_2)	0000 0110	-4.8524933639E-09
16	R 2(2, 0F_2)	0000 2000	-2.7018916009E-06

Table 4: Effective dipole moment parameters for the $\{2\nu_2+2\nu_4-\nu_2,\ 2\nu_2+\nu_3-\nu_2\}$ bands.

	Tensorial nomenclature		Parameter value
	Rotational	Vibrational	
1	$R\ 0(\ 0, 0A_1)$	0100 0202	3.9825129095E-04
2	$R\ 0(\ 0, 0A_1)$	0100 0210	8.5008049280E-03
3	$R\ 0(\ 0, 0A_1)$	0100 0202	6.5544003405E-06
4	$R\ 0(\ 0, 0A_1)$	0100 0210	7.9030718238E-05
5	$R\ 0(\ 0, 0A_1)$	0100 0202	-4.4623481744E-04
6	$R\ 0(\ 0, 0A_1)$	0100 0210	1.2930872868E-02
7	$R\ 0(\ 0, 0A_1)$	0100 1002	-4.6917331225E-03
8	$R\ 0(\ 0, 0A_1)$	0100 1010	2.4241217720E-03
9	$R\ 1(\ 1, 0F_1)$	0100 0210	-1.4446087275E-05
10	$R\ 1(\ 1, 0F_1)$	0100 0210	2.0583793143E-05
11	$R\ 1(\ 1, 0F_1)$	0100 0210	-2.4295434890E-08
12	$R\ 1(\ 1, 0F_1)$	0100 0210	6.1335719221E-07
13	$R\ 1(\ 1, 0F_1)$	0100 0210	-1.8777757468E-05
14	$R\ 1(\ 1, 0F_1)$	0100 0210	3.0644918638E-05
15	$R\ 1(\ 1, 0F_1)$	0100 1002	3.2123332254E-05
16	$R\ 1(\ 1, 0F_1)$	0100 1002	3.4243832575E-05
17	$R\ 1(\ 1, 0F_1)$	0100 1002	-5.2783161222E-05
18	$R\ 1(\ 1, 0F_1)$	0100 1002	-2.0547145593E-05
19	$R\ 1(\ 1, 0F_1)$	0100 1002	3.2786033893E-06
20	$R\ 1(\ 1, 0F_1)$	0100 1010	4.8417050701E-04
21	$R\ 1(\ 1, 0F_1)$	0100 1010	2.4135565610E-04
22	$R\ 1(\ 1, 0F_1)$	0100 2100	6.9831133618E-05
23	$R\ 1(\ 1, 0F_1)$	0100 2100	2.7944989174E-04
24	$R\ 2(\ 2, 0E\ )$	0100 1010	1.1388797951E-07
25	$R\ 2(\ 2, 0F_2)$	0100 1010	1.6758890863E-07
26	$R\ 2(\ 0, 0A_1)$	0100 1010	-3.1635728036E-07
27	$R\ 2(\ 2, 0E\ )$	0100 1010	3.0201035785E-07
28	$R\ 2(\ 2, 0F_2\ )$	0100 1010	-6.7979486512E-09

Table 5: Effective dipole moment parameters for the {ν_2+3ν_4-ν_4, ν_2+ν_3+ν_4-ν_4} bands.

	Tensorial nomenclature		Parameter value
	Rotational	Vibrational	
1	R 0(0, 0A_1)	0001 0103	4.2413135847E-04
2	R 0(0, 0A_1)	0001 0103	2.7477468633E-05
3	R 0(0, 0A_1)	0001 0103	5.0088447964E-04
4	R 0(0, 0A_1)	0001 0103	-1.2620967754E-05
5	R 0(0, 0A_1)	0001 0103	4.7003806247E-04
6	R 0(0, 0A_1)	0001 0103	6.4939084452E-05
7	R 0(0, 0A_1)	0001 0103	1.7797635608E-06
8	R 0(0, 0A_1)	0001 0111	-1.5473534628E-02
9	R 0(0, 0A_1)	0001 0111	-3.0138555124E-04
10	R 0(0, 0A_1)	0001 0111	-1.6398372407E-05
11	R 0(0, 0A_1)	0001 0111	2.5471384745E-04
12	R 0(0, 0A_1)	0001 0111	7.8534831544E-05
13	R 0(0, 0A_1)	0001 0111	-2.0691429033E-05
14	R 0(0, 0A_1)	0001 0111	-1.9854225634E-04
15	R 1(1, 0F_1)	0001 0111	2.2599131901E-05
16	R 1(1, 0F_1)	0001 0111	-3.8669830582E-05
17	R 1(1, 0F_1)	0001 0111	9.1638928149E-07
18	R 1(1, 0F_1)	0001 0111	-6.7549134470E-07
19	R 1(1, 0F_1)	0001 0111	2.9523535789E-07
20	R 1(1, 0F_1)	0001 0111	9.7740749402E-07
21	R 1(1, 0F_1)	0001 0111	-5.7925405576E-07
22	R 1(1, 0F_1)	0001 0111	3.8835519379E-07
23	R 1(1, 0F_1)	0001 0111	1.2693515619E-06
24	R 1(1, 0F_1)	0001 0111	1.1521893674E-06
25	R 1(1, 0F_1)	0001 0111	-5.5755866620E-08
26	R 1(1, 0F_1)	0001 0111	-4.1284363860E-07
27	R 1(1, 0F_1)	0001 0111	-4.6669243132E-07
28	R 1(1, 0F_1)	0001 0111	4.8599003861E-07
29	R 1(1, 0F_1)	0001 0111	5.2493460965E-08
30	R 1(1, 0F_1)	0001 0111	-6.2965529693E-07
31	R 1(1, 0F_1)	0001 0111	-8.3742085981E-07
32	R 1(1, 0F_1)	0001 0111	-7.7632490926E-07
33	R 1(1, 0F_1)	0001 0111	1.2083069804E-06
34	R 1(1, 0F_1)	0001 0111	-6.9909391873E-07

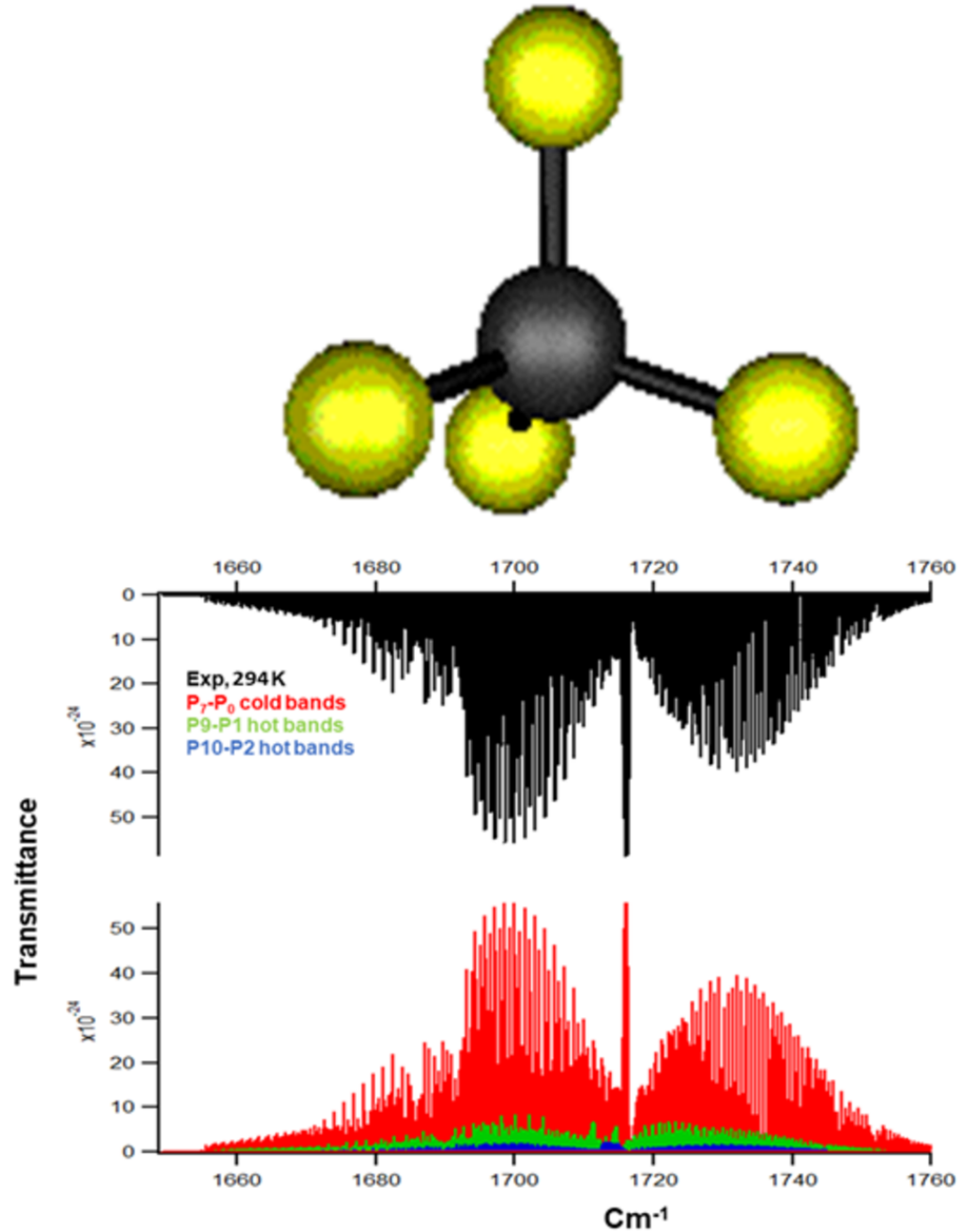
1660
1680
1700
1720
1740
1760
0
10
20
30
40
50
x10-24
Exp, 294K
P7-P0 cold bands
P9-P1 hot bands
P10-P2 hot bands
Transmittance
Cm-1